Historical diamond mine waste reveals carbon sequestration resource in kimberlite residue

T.R. Jones [a,*], J. Poitras [b], D. Paterson [c], G. Southam [b]

[a] WH Bryan Mining Geology Research Centre, Sustainable Minerals Institute, The University of Queensland, Indooroopilly, QLD 4068, Australia
[b] School of Earth & Environmental Sciences, The University of Queensland, St. Lucia, QLD, 4072, Australia
[c] The Australian Synchrotron (ANSTO), Clayton, Victoria 3168, Australia

ARTICLE INFO

ABSTRACT

Mined sub-aerially stored kimberlite provided a natural laboratory in which to examine the potential for carbon sequestration in ultramafic materials. A 15 cm hand sample of ~50-year-old 'cemented' coarse residue deposit (CRD) collected from a cemented surface layer in the Cullinan Diamond Mine tailings in Gauteng, South Africa, demonstrated the encouraging effects of weathering on mineral carbonation of kimberlite. The examination of petrographic sections using light microscopy, X-ray fluorescence microscopy (XFM) and backscatter electron – energy dispersive spectroscopy demonstrated that weathering produced extensive, secondary Ca/Mg carbonates that acted as an inter-granular cement, increasing the competency of the CRD, i.e., producing a hand sample. Nearly every grain in the sample, including primary, un-weathered angular carbonate clasts were coated in secondary, μm- to mm-scale carbonate layers, which are interpreted as secondary materials. DNA analysis of an internal, aseptic sample of secondary carbonate revealed that the weathered kimberlite hosts a diverse microbiome consistent with soils, metal cycling and hydrocarbon degradation that was found within the secondary carbonate, interpreted as a biomaterial. The formation of secondary carbonate demonstrates that 'waste kimberlite' from diamond mining can serve as a resource for carbon sequestration.

1. Introduction

As global energy requirements increase to match Earth's rising population, so too do our emissions, resulting in an increase in the amount of CO_2 in our atmosphere and amplifying Earth's natural greenhouse effect (IPCC, 2021). There are diverse natural carbon sequestration processes that can draw CO_2 out of the atmosphere and 'lock' it away into a more stable form. Soils, forests, and oceans, all have the capacity to sequester gigatons of CO_2 annually as organic and inorganic biomaterials, and these natural processes may provide lessons for the development of novel biotechnological approaches aimed at sequestering CO_2. Of these processes, mineral carbonation is the only process that produces a geologically stable carbon sink (IPCC, 2021).

Carbon sequestration via mineral carbonation within mined mafic/ultramafic tailings has been suggested as a safe, stable way for mines to offset their carbon emissions (Mervine et al., 2018). The mechanisms by which carbon is locked into a mineral form is dependent on many variables, e.g., a source of carbon, alkalinity generation, and mineral dissolution/sources of cations (Li et al., 2019; Power et al., 2013). This latter factor is crucial as it is mineral breakdown that supplies the cations that will go on to precipitate as carbonates. Ultramafic rocks (peridotites, serpentinites, and kimberlites) serve as possible, alkaline hosts for carbon sequestration via carbon mineralisation by capturing and preserving atmospheric CO_2 in a stable mineral form. This occurs through the reaction of a CO_2 source with the suitable cations released from these ultra-mafic rocks during weathering (Power et al., 2014). In diamond deposits, the carbonisation process is reflected by the surficial transformation of blue ground (non-altered/competent) kimberlite into yellow ground (weathered/friable) kimberlite. This occurs naturally when the primary blue ground is exposed to Earth's surface conditions, i. e., occurring within 10's of meters of the Earth's surface, where the kimberlite is impacted by atmospheric interaction/meteoric water and biology (Fairbairn and Robertson, 1966; Mitchell, 2008; Sparks, 2013).

Weathering of kimberlite pipes creates vertical zoning that depletes the surficial zone of CaO, MgO and CO_2, often re-precipitating these materials as calcite and dolomite in deeper parts of the kimberlite (Ruotsala, 1975). Remarkably, the historical weathering of kimberlite under surface conditions can occur within decadal time scales. This fact

was exploited during early 'blue ground' diamond processing – where exposing un-altered kimberlite to surface conditions for as little as a few years resulted in the production of enough alteration to recover diamonds from these partially-weathered materials (Boshoff et al., 2005). Kimberlite weathering is primarily understood to be a geological, i.e., abiotic, process typically involving wetting and drying swelling clays, and rainfall-induced carbonic acid dissolution (Morkel and Vermaak, 2006). This weathering accelerates geochemical cycling and attacks the primary mineralogy, such as the olivine and monticellite (rxns 1 and 2) that is prominent in the kimberlites mined at the Cullinan diamond mine (Dongre and Tappe, 2019). This carbonic acid weathering can be accelerated by heterotrophic microbial activity, which elevates the concentration of carbon dioxide, and therefore carbonic acid in soils (Enoch and Dasberg, 1971).

$$Mg_2SiO_4 + 4\,CO_2 + 4\,H_2O \rightarrow 2\,Mg^{2+} + 4\,HCO_3^- + H_4SiO_4 \quad (1)$$

$$CaMgSiO_4 + 4\,CO_2 + 4\,H_2O \rightarrow Ca^{2+} + Mg^{2+} + 4\,HCO_3^- + H_4SiO_4 \quad (2)$$
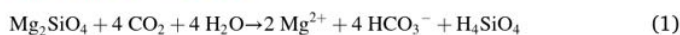
When combined with the release of divalent cations, continued acid weathering of ultramafic material, e.g., serpentine (Dongre and Tappe, 2019; rxn 3) will increase pH,

$$Mg_3Si_2O_5(OH)_4 + 6\,H^+ \rightarrow 3\,Mg^{2+} + 2\,SiO_2 + 5\,H_2O \quad (3)$$
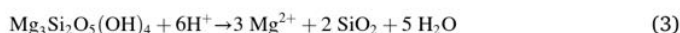
promoting mineral carbonation. Water-rock interactions are also known to support the growth of the biosphere and the formation of soils (Kump et al., 2000). Therefore, the alteration of kimberlite into yellow ground will intuitively involve both abiotic and microbially catalysed reactions (Power et al., 2011).

Microorganisms, in fact, have a massive impact on surface and subsurface environments, reaching up to 10^9 cells/g soil (Whitman et al., 1998). Living in diverse environments, microbes utilise a range of metabolic pathways to create the energy required for life. This includes securing the elements they need to grow and divide, i.e., C, N, P and S, with P the typically limiting nutrient (Welch et al., 2002). Bacteria-mineral interactions occur at nanometer- to micrometer-scales, where they impact the chemistry of this interface via inorganic, e.g., carbonic acid, and organic acid formation, which can break down mineral substrates (Chen et al., 2006; Dong et al., 2022; Watling, 2008). Alongside accelerated weathering via bacterial activity, different microorganisms can aid in the precipitation of minerals by modifying their environment via biogeochemical cycling (Dong et al., 2022; Mitchell, 2008).

In suitable environments possessing high pH conditions and soluble divalent cations, microorganisms can promote the formation of carbonate minerals. Specifically, microbially induced carbonate precipitation (MICP) in weathered kimberlite residue can potentially occur via a combination of oxygenic photosynthesis, dissimilatory sulphate reduction and ammonification (Stal, 2012; Vousdoukas et al., 2007).

Historical mines are excellent natural laboratories to examination how tailings evolve under natural weathering conditions, offering an insight into early alteration reactions occurring in kimberlite. By looking at historical tailings we aim to improve our understanding of kimberlite weathering under Earth surface conditions. Elemental mapping and DNA analysis of this weathered yellow ground will reveal the extent to which this reactive material is transformed under surface conditions, the resulting biogeochemical features produced via weathering, and its capacity to support a microbiome. These processes are crucial to understanding the capacity to which kimberlitic material can support carbonate precipitation post diamond extraction; providing insight into any ultramafic hosted carbon sequestration ventures.

2. Materials and methods

The Cullinan Diamond Mine offers a rare oppurtunity to observe the natural alteration of tailings at surface conditions on a decadal time-scale, as ~50 year old processed material has been been left 'untouched' by further mining activity. Previously known as the Premier Mine, the Cullinan Diamond Mine (Fig. 1) is located in Gauteng, ZAF, ~ 40 km east of Pretoria. Open-pit extraction commenced at the site in 1903, prior to transitionining to underground extraction in 1946. The Premier kimberlite pipe around which this mine operates is a large (~ 32 ha) diamond bearing diatreme with a complex emplacement history via the presence of both coherent magmatic and volcaniclastic infill (Bartlett, 1994; Tappe et al., 2018). One 15 cm hand-sample of cemented, surface exposed CRD (Fig. 1C) was allowed to be collected for study.

Due to the generally friable nature of this material, a ~ 3 cm sub-sample was vacuum embedded using Epo-Tek 301–2 resin prior to any cutting for materials characterisation. This two-component, low viscosity resin was used with the aim of preserving any delicate, secondary carbonate structures. The embedded rock was then cut and polished producing two, 30 μm thick petrographic thin sections for petrology, X-ray Fluorescence Microscopy (XFM) and Scanning Electron Microscopy (SEM).

Plane polarised light microscopy was performed using a Leica DM6000M automated microscope. Elemental mapping of a thin section was performed using synchrotron X-ray Fluorescence Microscopy (XFM) using 12.9 KeV incident energy and processed using GeoPIXE™. Areas consisting of secondary Ca minerals, identified using XFM (Fig. 2), were also examined using BSE-SEM (Fig. 3)-Energy-Dispersive X-ray Spectroscopy (EDS) to ascertain elemental abundances, of Ca, Mg, C and O, for carbonate composition. Unweathered kimberlite clasts, secondary carbonate and pore space by volume was approximated by ratioing the three components of the 2-D XFM images in Fig. 2B by measuring the mass of each fraction and ratioing to the area (mass) to total mass/area, i.e., 100%

The carbonate associated biosphere, i.e., cells, were exposed from within the carbonate cement by immersing a 10 g sub-sample, collected adjacent to the DNA sample in 100 ml $2.5\%_{(aq)}$ HCl for 3 min to partially dissolve the carbonate. The HCl slurry was then vacuum filtered (0.45 μm) and the solids + bacteria resuspended in 20 ml, $2.5\%_{(aq)}$ glutaraldehyde fixative for 24 h. The fixed sample was then processed using an ethanol dehydration series (20%, 40%, 60%, 80%, 3 × 100%), and dried using hexamethyldisilane in ethanol (33%, 66%, 100%) then in air, to preserve biomass. The dried sample was immobilised on 12.5 mm Al-pin stub with a carbon sticky and placed in a vacuum oven (40 °C) overnight, plasma cleaned using an Evactron 25 De-Contaminator RF Plasma Cleaning System and Pt-coated (15 nm) using a Quorum Q150TS metal coater prior to electron microscopy. All Scanning Electron Microscopy (SEM) was undertaken using a JOEL JSM-7100 Field Emission Scanning Electron Microscope (FE-SEM), equipped with a JEOL 129 eV resolution silicon drift detector (SDD) for EDS. The SEM was operated at 20 KeV for BSE imaging and EDS measurements, and at 2 KeV for secondary electron imaging.

For molecular biological analyses, the non-embedded remnant of the hand sample was carefully broken open in a sterilised laminar flow cabinet to reveal a fresh internal surface for sampling. This was done to avoid sampling extraneous DNA that may have contaminated the outer surface. A 1 g sample of friable, internal secondary carbonate was scraped from the sample using a sterilised spatula and submerged in LifeGuard® Soil Preservation Solution (QIAGEN) for preservation. This friable cement was targeted for microbial sampling as it was formed after the kimberlitic material had been deposited as CRD, and will therefore provide a DNA snapshot of any microorganism that are coeval with the carbonate material.

DNA extraction was caried out using a laminar flow cabinet to recover material of freshly exposed rock surfaces. The whole sample was cracked in half using sterile tools and ~ 2 g of material was scraped into a tube for DNA extraction. DNA was extracted from 50 to 200 mg of sample using 0.1 diameter glass beads for preliminary bead beating (BioSpec Products #11079101) on a Powerlyser 24 homogeniser. Sample is added to a bead tube filled with 850 μl of CD1 (Qiagen cat
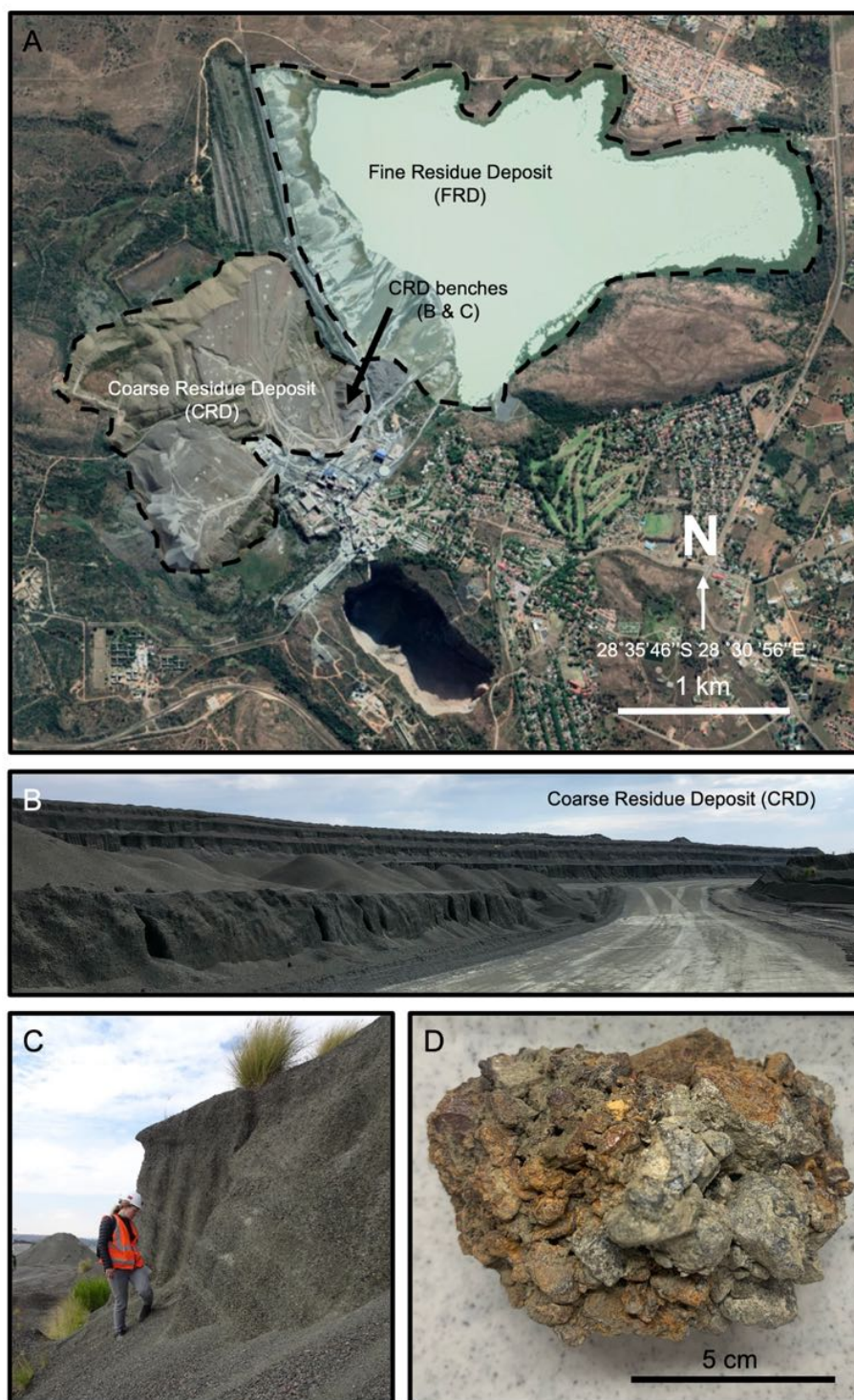
Fig. 1. A) Google Earth image of the Cullinan Diamond Mine – showing the Fine Residue Deposit, the Coarse Residue Deposit, and the pit to the south. B) A road along a CRD bench. C) Close up of a bench indicating it's competency. D) Hand sample of cemented Cullinan CRD.

#47016) and mixed by vortex. Tubes were heated to 65 °C for 10 min and then beat for 5 min at 2000 RPM and centrifuged for one minute at 15000 g. Resulting lysate is then transferred to a new collection tube for PCR amplification with a final elution volume of 50 μl.

Amplification of the V6 to V8 regions of the 16 s rRNA gene using the universal primers 926f and 1392r (14) adapted to contain Illumina-specific adapter sequences (adapter sequences in capitals): 926F: 5′-TCGTCGGCAGCGTCAGATGTGTATAAGA GACAGaaactyaaakgaattgacgg-3′ and 1392wR: 5′-GTCTCGTGGG CTCGGGTCTCGTGGGCTCGGA

GATGTGTATAAGAGACAG acgggcggtgtgtrc-3′. Libraries were prepared as described by Illumina (#15044223 Rev. B), except that Q5 Hot Start High-Fidelity polymerase and PCR mastermix were used (New England Biolabs, Ipswich, MA, USA). Resulting PCR amplicons were purified using Agencourt AMPure XP beads (Beckman Coulter, Brea, CA, USA). Purified DNA was indexed with unique 8-bp barcodes using the Illumina Nextera XT 384 Index Kit A-D (Illumina FC-131-1002) in standard PCR conditions with NEBNext® Ultra™ II Q5® Mastermix. Indexed amplicons were pooled together in equimolar concentrations and sequenced

on a MiSeq Sequencing System (Illumina) using paired end sequencing with V3 300 bp chemistry in accordance with the manufacturer's protocol at the Australian Centre for Ecogenomics, The University of Queensland.

Sequences were processed using the method by Gagen et al. (2018) except with updated MOTHUR Version 1.45.3 (Schloss et al., 2009) and the updated SILVA v138 database (Quast et al., 2013). The reads of the sample started with 7404 sequences before cleaning and grouping. Briefly, ambiguous sequences were filtered, trimmed to 250 base pairs, and aligned to the SILVA database resulting in 425 unique sequences. Chimeric sequences were removed using uchime, resulting in 9.2% chimeric sequences. A total of 118 unique sequences were then classified using the SILVA database whereafter eukaryotes, chloroplasts, mitochondria and unknowns were removed. Sequences were grouped into operational taxonomic units (OTUs) to 97% similarity, resulting in 103 OTUs. Representative sequences of major OTUs were compared to publicly available sequences using the Nucleotide Basic Local Alignment Search Tool (BLASTn) at the NCBI and the non-redundant nucleotide collection, excluding uncultured selections. As a hand sample, genera consistent with human skin, i.e., *Staphylococcus*, *Cutibacterium*, *Corynebacterium* and *Peptoniphilus* were considered contaminants, and not examined further.

3. Results

Petrology and XFM of the cemented sample revealed a substantial network of calcium rich material possessing draping textures and surrounding >90% of the individual grains making up the CRD (Fig. 2AB).
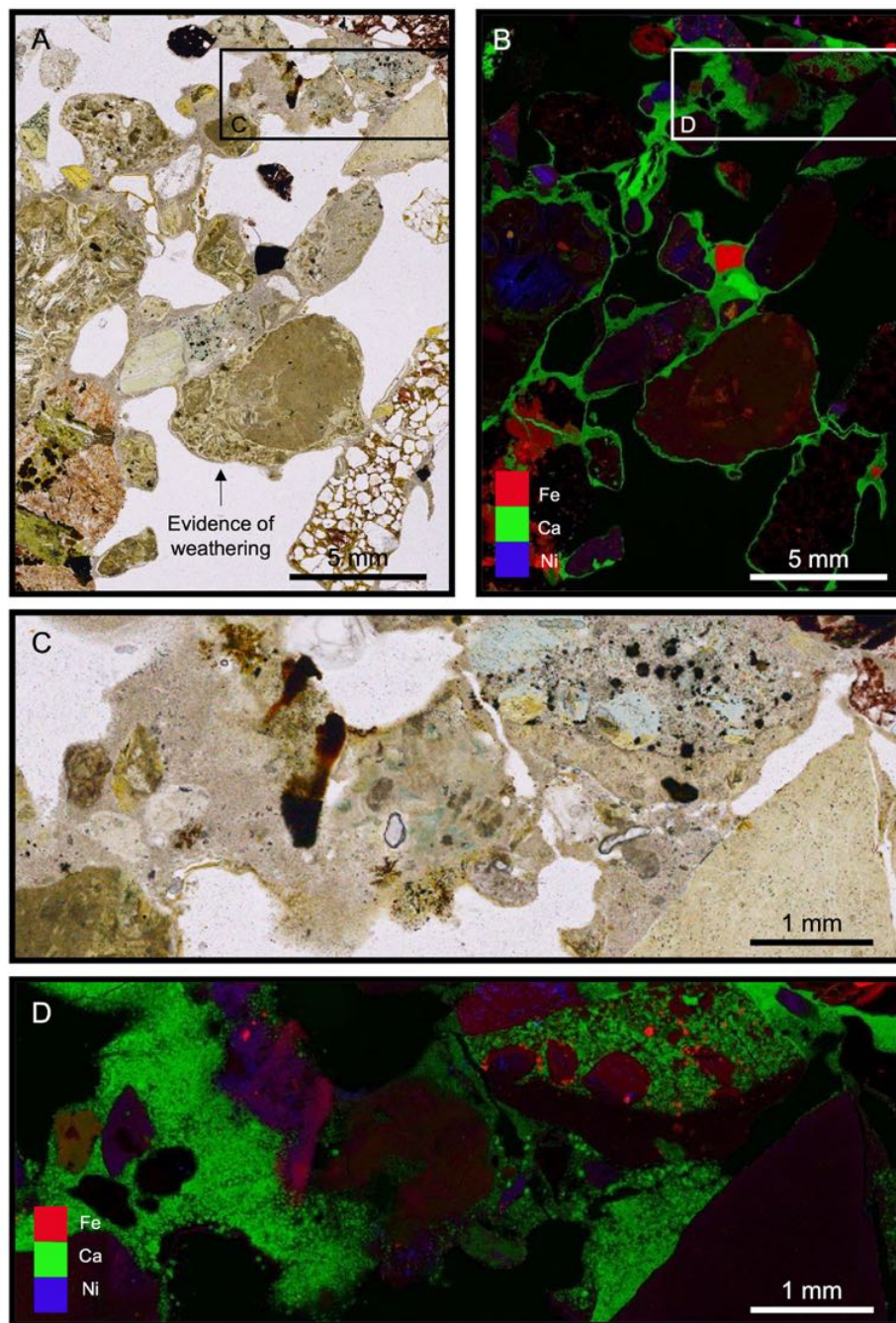

Fig. 2. Representative PPL (A) and XFM (B) images of the CRD in thin section showing discreet grains encased in a calcium rich cement. High-resolution microscopy in both PPL (C) and XFM (D) revealed a granular, speckled texture within the secondary calcium rich cement.
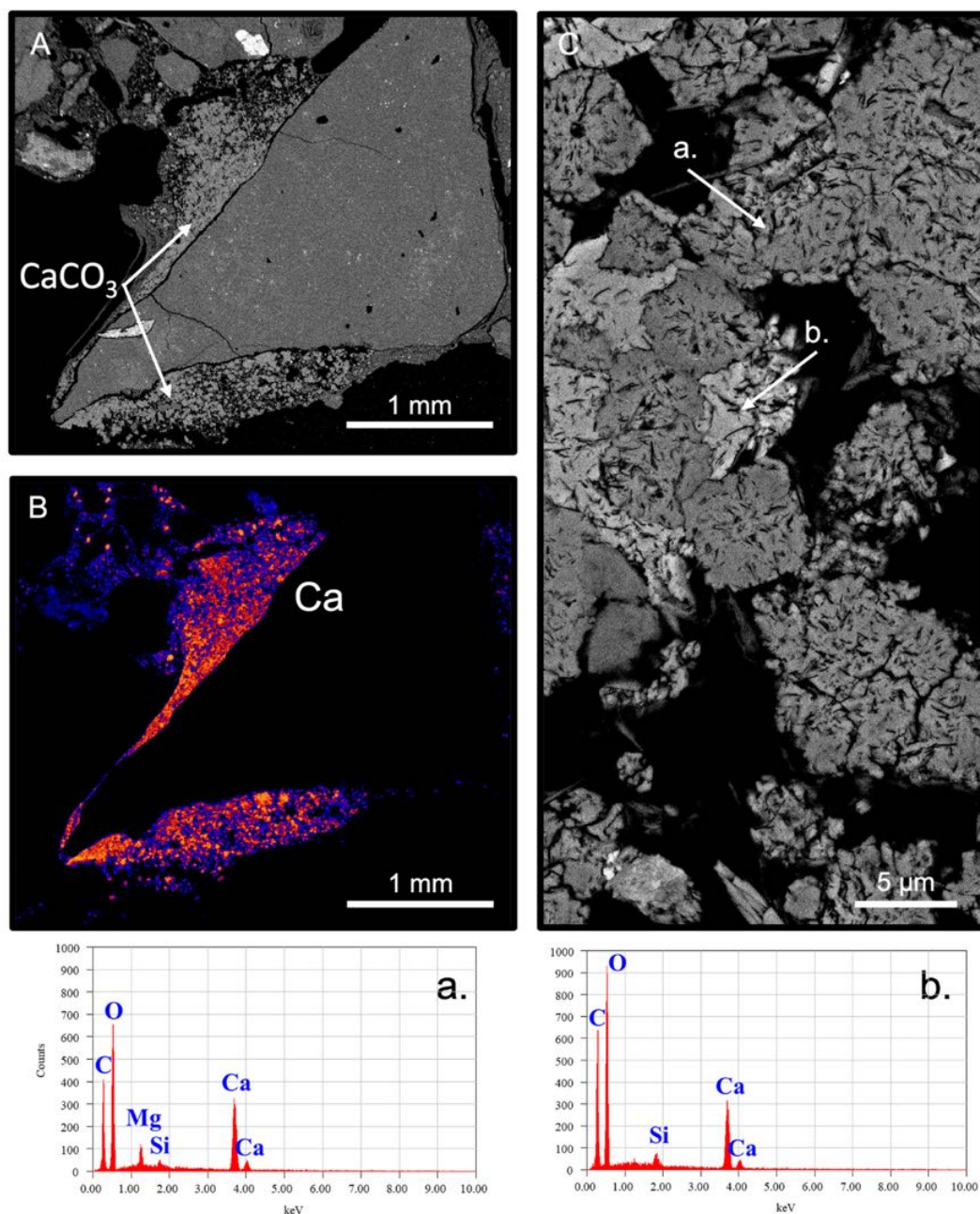
Fig. 3. A) BSE-SEM showing the newly formed carbonate cement surrounding a discreet grain and B) XFM of the same area showing the concentration of calcium within the carbonate cement. Note, grey scale, atomic mass differentiation of Mg—Ca carbonate (a; darker regions), and Ca carbonate (b; lighter regions).

Based on XFM imaging, the cemented CRD comprised 55.3% primary minerals, 32.8% void space and 11.8% secondary, carbonate cement. Scaled for density (calcite/aragonite = 2.75 g/cm^3, kimberlite = 3.3 g/cm^3), this indicates that the secondary carbonate constitutes 16.39 wt% of the system. This secondary calcium cement was easily differentiated from the brighter, discrete, and homogenous, primary calcium-bearing minerals observed within the sample. The granular texture observed within the secondary 'calcium' cement ranged from ~1 μm to ~50 μm (Fig. 2D, Fig. 3B) demonstrating abundant nucleation sites that produced a speckled texture in the secondary carbonate (Fig. 3a) and allowed for the intergrowth of carbonate minerals with differing Ca:Mg ratios on a localised scale. All observable Fe and Ni within the sample was housed within unweathered, primary kimberlite minerals. EDS spectroscopy demonstrated that the calcium cement binding the CRD material together was composed of C, O, Ca +/− minor Mg, which was interpreted as carbonate, with the spectra showing corroborating EDS atomic abundances (Fig. 3AB). Along with the calcium carbonate observed using XFM and BSE-SEM-EDS, there are also regions of Ca—Mg carbonate (Fig. 3A).

Mild acid treatment, using pH 4 HCl, dissolved carbonate coating the weathered CRD material, which exposed abundant, previously entombed bacteria (Fig. 4) that were 'hidden' within the carbonate. These previously encapsulated bacteria are shown to be inter-grown with the carbonate, intuitively playing a role in carbon mineralisation.

The 16S rDNA microbial community at >1% frequency is presented at the taxonomic rank of Family where possible, and at the rank of Order for the unclassified populations: Sphingomonadaceae (20%), Actinobacteria-unclassified (19%), Streptococcaceae (16%), Propionibacteriaceae (14%), Staphylococcaceae (7%), Anaerolineaceae (5%), SC-I-84 (5%), Magnetospiraceae (5%), Burkholderiales-unclassified (5%), Rubinisphaeraceae (4%). At the genus level, the bacterial make-up of the most prominent OTUs within this CRD sample exhibited a diverse range of autotrophic and heterotrophic microbial metabolic pathways being utilised within the environment. Several anerobic and facultative bacteria are among the most populous genera observed (*Methanobrevibacter* sp. ~ 4.5%, *Sediminispirochaeta* sp. ~ 3.9%, *Microscillaceae* sp. ~ 3.05%, *Methanoperedens* sp. ~ 2.9%, *Klebsiella* sp. ~ 2.5%, and *Prevotella* sp. ~ 1.9%). Four phototrophic genera were prominent in the microbial community, three aerobic (*Oscillatoria* sp. ~4.2%, *Porphyrobacter* sp. ~2.6%, and *Blastomas* sp. ~2.1%), and one anaerobic (*Rhodobacter* sp. ~4.2%).
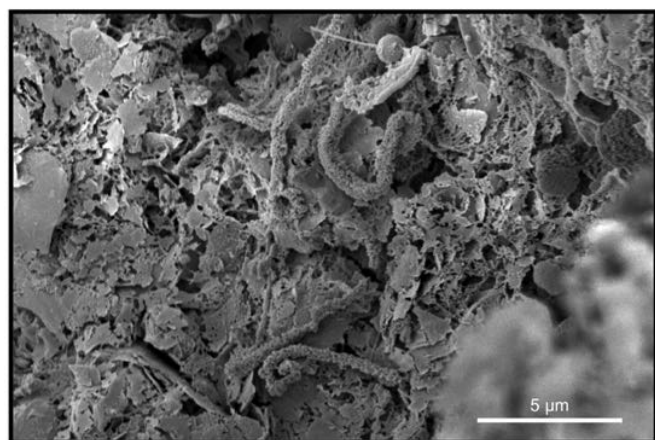

Fig. 4. SE-SEM of acid treated material revealing several previously entombed rod-shaped and filamentous bacteria from within the secondary carbonate cement.

4. Discussion

The abundance and diversity of bacteria within this cemented residue suggests a microbial role in weathering ultramafic kimberlitic material and mineral carbonation. The cemented material possessed an array of phototrophic/heterotrophic biofilm producers (e.g., Sphingomonadaceae) and symbiotic nitrogen fixers (*Actinobacteria*) (Li et al., 2019) consistent with the low nitrogen levels in kimberlite. Organic acid production from fermenters (Propionibacteriaceae and Streptococcaceae; Delwiche, 1957; Giassi et al., 2016) and chemolithotrophs (Anaerolineaceae) would enhance mineral weathering, e.g., phosphorous acquisition, and potentially promoted carbonate deposition in these alkaline materials (Lory, 2014). The presence of iron-bearing minerals (Fig. 2D circle) may be responsible for the occurrence of Magnetospiraceae, which are common to mafic rocks where they contribute to the biogeochemical cycling of iron. This is consistent with the establishment of periodic reducing conditions, likely as microenvironments, in this at-surface environment (Kulichevskaya et al., 2015; Molari et al., 2020). Given the colonisation of grasses observed on site (data not shown), taxa consistent with soil formation and decomposing plant material were found (SC-I-84, Actinobacteria, Burkholderiales and Streptococcaceae; Pershina et al., 2015; Ningthoujam et al., 2009; Vandamme and Coenye, 2004; Giassi et al., 2016). Plant material (see grasses in Fig. 1C) as well as the occurrence of hydrocarbons in diamond bearing materials (Sobolev et al., 2019) are consistent with the presence of hydrocarbon-degrading bacteria (Anaerolineaceae Rubinisphaeraceae and Sphingomonadaceae; Liang et al., 2015, Byrne, 2021; Oh and Choi, 2019).

This microbial snapshot was extracted from the friable secondary cements from within the sample, and therefore represent the community present and active during the precipitation of the carbonate material. The relationship between the secondary carbonate and microbial community observed also aligns with the observation of microorganisms using Secondary Electron SEM. As the observation of these cells were only possible post acid treatment, this indicates that the microorganisms were previously bound within the carbonate and hidden from view.

While the natural rate of weathering since extraction is impossible to ascertain, the formation of secondary carbonates will have occurred post processing, resulting in the formation of carbonate duricrusts comparable to the biological cements produced in stromatolites and beachrock (McCutcheon et al., 2016; McCutcheon et al., 2017). The precipitation of Ca/Mg carbonate minerals has bound the CRD grains of kimberlite together, serving as a cement. This has resulted in the consolidation of the once loose material, creating a level of competency that allows metre scale benches to maintain near vertical faces (Fig. 1C). The source of carbon is interpreted to be the atmosphere as there was no evidence of weathering of primary carbonate, combined with the diverse biosphere, including phototrophic activity, soil formation processes, i.e., mineral weathering, and organic matter recycling within the carbonate cemented CRD, support the atmospheric drawdown of CO_2.

The presence of post depositional inter-grain cement confirms that crushed kimberlite, such as that produced via the mining of diamonds, can accommodate the formation of secondary carbonate minerals. The carbonate cement observed within the Cullinan CRD has occurred naturally on a decadal timescale, likely catalysed in part by the presence of microorganisms. The diversity and abundance (Fig. 4) of bacteria extracted from the secondary cement, and visible only after acid dissolution of carbonate, suggests the involvement of these organisms in the development of these secondary carbonate minerals. Microorganisms have been observed to induce carbonate precipitation by acting as nucleation sites under saturating conditions (McCutcheon et al., 2016), and via geochemical alterations, with both heterotrophic and photosynthetic bacteria found in the cemented CRD likely mediating carbonate precipitation (Dittrich et al., 2003; Guo and Riding, 1992; Heath et al., 1995; Power et al., 2011; Rodriguez-Navarro et al., 2007).

The natural tendency for weathering and secondary mineral

precipitation within kimberlitic material may serve as the platform for accelerating this novel carbon sequestration process for the diamond mining industry. In South Africa, where mines are on the electricity grid, the dilute reservoir of carbon dioxide in the atmosphere is the only direct source of CO_2, and can only be captured, economically at these remote sites via the biosphere.

5. Conclusions

Access to kimberlitic material mined approx. 50 years ago (from ca. 1970) offered an insight into natural, mineral carbonation processes, and how contemporary kimberlite mines may be expected to react over the coming decades. Weathering of coarsely processed kimberlitic material from Cullinan supported a diverse microbial community and produced secondary carbonate minerals. The occurrence of photosynthetic bacteria and grasses suggests these organisms may have served as a catalyst and a conduit for the transformation of atmospheric CO_2 into (Ca, Mg) carbonates. The observation of these carbonates in historical kimberlite residue exemplifies the capacity for these anthropogenic deposits to sequester carbon, providing a novel carbon capture process for the diamond industry.

Declaration of Competing Interest

The authors declare the following financial interests/personal relationships which may be considered as potential competing interests:

Gordon Southam reports financial support was provided by De Beers Group Services RSA Pty Ltd. Gordon Southam reports financial support was provided by Australian Nuclear Science and Technology Organisation. Gordon Southam reports a relationship with De Beers Group Services RSA Pty Ltd. that includes: funding grants.

Data availability

Data will be made available on request.

Acknowledgements

References

Bartlett, P., 1994. Geology of the Premier diamond pipe. In: Proceedings of the XVth CMMI Congress, South African Institute of Mining and Metallurgy, Johannesburg, p. 214.

Boshoff, E.T., Morkel, J., Vermaak, M.K.G., 2005. Accelerated kimberlite weathering-the role of cation type on the settling behaviour of fines: the. J. S. Afr. Inst. Min. Metall. 105, 163–166.

Byrne, E., 2021. Hydrocarbon Biodegradation and Microbial Community Composition in Freshwater Systems and Enriched Cultures. MSc thesis.. Michigan Technological University Digital Commons@Michigan Tech.

Chen, Y., Rekha, P., Arun, A., Shen, F., Lai, W.-A., Young, C., 2006. Phosphate solubilizing bacteria from subtropical soil and their tricalcium phosphate solubilizing abilities. Appl. Soil Ecol. 34, 33–41.

Delwiche, E.A., 1957. Family XI. Propionobacteriaceae Delwiche, fam. nov. In: Breed, R. S., Murray, E.G., Smith, N.R. (Eds.), Bergey's Manual of Determinative Bacteriology, 7th ed. The Williams and Wilkins Co, Baltimore, MD, p. 569.

Dittrich, M., Muller, B., Mavrocordatos, D., Wehrli, B., 2003. Induced calcite precipitation by cyanobacterium *Synechococcus*. Acta Hydrochim. Hydrobiol. 31, 162–169.

Dong, H., Huang, L., Zhao, L., Zeng, Q., Liu, X., Sheng, Y., Shi, L., Wu, G., Jiang, H., Li, F., Zhang, L., 2022. A critical review of mineral–microbe interaction and co-evolution: mechanisms and applications. Natl. Sci. Rev. 9 (10) p.nwac128.

Dongre, A., Tappe, S., 2019. Kimberlite and carbonatite dykes within the Premier diatreme root (Cullinan Diamond Mine, South Africa): new insights to mineralogical-genetic classifications and magma CO_2 degassing. Lithos 338–339, 155–173.

Enoch, H., Dasberg, S., 1971. The occurrence of high CO_2 concentrations in soil air. Geoderma 6, 17–21.

Fairbairn, P., Robertson, R., 1966. Stages in the tropical weathering of kimberlite. Clay Miner. 6, 351–370.

Gagen, E.J., Levett, A., Shuster, J., Fortin, D., Vasconcelos, P.M., Southam, G., 2018. Microbial diversity in actively forming iron oxides from weathered banded iron formation systems. Microbes Environ. 33, 385–393.

Giassi, V., Kiritani, C., Kupper, K.C., 2016. Bacteria as growth-promoting agents for citrus rootstocks. Microbiol. Res. 190, 46–54.

Guo, L., Riding, R., 1992. Aragonite laminae in hot water travertine crusts, Rapolano Terme, Italy. Sedimentology 39, 1067–1079.

Heath, C.R., Leadbeater, B.C.S., Callow, M.E., 1995. Effect of inhibitors on calcium carbonate deposition mediated by freshwater algae. J. Appl. Phycol. 7, 367–380.

IPCC, 2021. In: Masson-Delmotte, V., Zhai, P., Pirani, A., Connors, S.L., Péan, C., Berger, S., Caud, N., Chen, Y., Goldfarb, L., Gomis, M.I., Huang, M., Leitzell, K., Lonnoy, E., Matthews, J.B.R., Maycock, T.K., Waterfield, T., Yelekçi, O., Yu, R., Zhou, B. (Eds.), Climate Change 2021: the Physical Science Basis. Contribution of Working Group I to the Sixth Assessment Report of the Intergovernmental Panel on Climate Change. Cambridge University Press.

Li, L., Jeon, Y., Lee, S.-H., Ryu, H., Santo Domingo, J.W., Seo, Y., 2019. Dynamics of the physiochemical and community structures of biofilms under the influence of algal organic matter and humic substances. Water Res. 158, 136–145.

Liang, B., Wang, L.Y., Mbadinga, S.M., Liu, J.F., Yang, S.Z., Gu, J.D., Mu, B.Z., 2015. *Anaerolineaceae* and *Methanosaeta* turned to be the dominant microorganisms in alkanes-dependent methanogenic culture after long-term incubation. AMB Express 5, 37.

Kulichevskaya, I.S., Ivanova, A.A., Detkova, E.N., Rijpstra, W.I.C., Damste, J.S.S. and Dedysh, S.N., 2015. Planctomicrobium piriforme gen. nov., sp. nov., a stalked planctomycete from a littoral wetland of a boreal lake. *International Journal of Systematic and Evolutionary Microbiology*, 65(Pt_5), pp.1659-1665.

Kump, L.R., Brantley, S.L., Arthur, M.A., 2000. Chemical weathering, atmospheric CO2, and climate.

Lory, S., 2014. The Family Streptococcaceae. In: Rosenberg, E., DeLong, E.F., Lory, S., Stackebrandt, E., Thompson, F. (Eds.), The Prokaryotes: Firmicutes and Tenericutes. Springer, Berlin Heidelberg, Berlin, Heidelberg, pp. 367–370.

McCutcheon, J., Nothdurft, L.D., Webb, G.E., Paterson, D., Southam, G., 2016. Beachrock formation via microbial dissolution and re-precipitation of carbonate minerals. Mar. Geol. 382, 122–135.

McCutcheon, J., Nothdurft, L.D., Webb, G.E., Shuster, J., Nothdurft, L., Paterson, D., Southam, G., 2017. Building biogenic beachrock: Visualizing microbially-mediated carbonate cement precipitation using XFM and a strontium tracer. Chem. Geol. 465, 21–34.

Mervine, E.M., Wilson, S.A., Power, I.M., Dipple, G.M., Turvey, C.C., Hamilton, J.L., Vanderzee, S., Raudsepp, M., Southam, C., Matter, J.M., Kelemen, P.B., 2018. Potential for offsetting diamond mine carbon emissions through mineral carbonation of processed kimberlite: an assessment of De Beers mine sites in South Africa and Canada. Mineralogy and Petrology 112 (2), 755–765.

Mitchell, R.H., 2008. Petrology of hypabyssal kimberlites: Relevance to primary magma compositions. J. Volcanol. Geotherm. Res. 174, 1–8.

Molari, M., Janssen, F., Vonnahme, T., Wenzhöfer, F., Boetius, A., 2020. Microbial communities associated with sediments and polymetallic nodules of the Peru Basin. Biogeosciences. https://doi.org/10.5194/bg-2020-11.

Morkel, J., Vermaak, M.K.G., 2006. The role of swelling clay in kimberlite weathering. Miner. Process. Ext. Metall. 115, 150–154.

Ningthoujam, D.S., Sanasam, S., Tamreihao, K., Nimaichand, S., 2009. Antagonistic activities of local actinomycete isolates against rice fungal pathogens. Afr. J. Microbiol. Res. 3, 737–742.

Oh, S., Choi, D., 2019. Microbial community enhances biodegradation of bisphenol A through selection of Sphingomonadaceae. Microb. Ecol. 77, 631–639.

Pershina, E., Valkonen, J., Kurki, P., Ivanova, E., Chirak, E., Korvigo, I., Provorov, N., Andronov, E., 2015. Comparative analysis of prokaryotic communities associated with organic and conventional farming systems. PLoS One 10, e0145072.

Power, I.M., Wilson, S.A., Dipple, G.M., Southam, G., 2011. Modern carbonate microbialites from an asbestos open pit pond, Yukon, Canada. Geobiology 9, 180–195.

Power, I.M., Harrison, A.L., Dipple, G.M., Wilson, S.A., Kelemen, P.B., Hitch, M., Southam, G., 2013. Carbon mineralization; From natural analogues to engineered systems. Rev. Mineral. Geochem. 77, 305–360.

Power, I.M., Wilson, S.A., Harrison, A.L., Dipple, G.M., McCutcheon, J., Southam, G., Kenward, P.A., 2014. A depositional model for hydromagnesite–magnesite playas near Atlin, British Columbia, Canada. Sedimentology 61, 1701–1733.

Quast, C., Pruesse, E., Yilmaz, P., Gerken, J., Schweer, T., Yarza, P., Peplies, J., Glöckner, F.O., 2013. The SILVA ribosomal RNA gene database project: improved data processing and web-based tools. Nucleic Acids Res. 41, D590–D596.

Rodriguez-Navarro, C., Jimenez-Lopez, C., Rodriguez-Navarro, A., Gonzalez-Munoz, M. T., Rodriguez-Gallego, M., 2007. Bacterially mediated mineralization of vaterite. Geochim. Cosmochim. Acta 71, 1197–1213.

Ruotsala, A.P., 1975. Alteration of the Finsch kimberlite pipe, South Africa. Economic Geology 70 (3), 587–590.

Schloss, P.D., Westcott, S.L., Ryabin, T., Hall, J.R., Hartmann, M., Hollister, E.B., Lesniewski, R.A., Oakley, B.B., Parks, D.H., Robinson, C.J., Sahl, J.W., Stres, B., Thallinger, G.G., Van Horn, D.J., Weber, C.F., 2009. Introducing mothur: open-

source, platform-independent, community-supported software for describing and comparing microbial communities. Appl. Environ. Microbiol. 75, 7537–7541.

Sobolev, N.V., Tomilenko, A.A., Bul'bak, T.A., Logvinova, A.M., 2019. Composition of rhydrocarbons in diamonds, garnet, and olivine from diamondiferous peridotites from the Udachnaya Pipe in Yakutia, Russia. Engineering 5, 271–278.

Sparks, R.S.J., 2013. Kimberlite volcanism. Annu. Rev. Earth Planet. Sci. 41, 497–528.

Stal, L.J., 2012. Cyanobacterial mats and stromatolites. In: *Ecology of cyanobacteria II.* Springer, Dordrecht, pp. 65–125.

Tappe, S., Dongre, A., Liu, C.-Z., Wu, F.-Y.J.G., 2018. 'Premier' evidence for prolonged kimberlite pipe formation and its influence on diamond transport from deep Earth. Geology 46, 843–846.

Vandamme, P., Coenye, T., 2004. Taxonomy of the genus Cupriavidus: A tale of lost and found. Int. J. Syst. Evol. Microbiol. 54, 2285–2289.

Vousdoukas, M.I., Velegrakis, A.F., Plomaritis, T.A., 2007. Beachrock occurrence, characteristics, formation mechanisms and impacts. Earth Sci. Rev. 85, 23–46.

Watling, H.R., 2008. The bioleaching of nickel-copper sulfides. Hydrometallurgy 91 (1–4), 70–88.

Welch, S.A., Taunton, A., Banfield, J.F., 2002. Effect of microorganisms and microbial metabolites on apatite dissolution. Geomicrobiology 19, 343–367.

Whitman, W.B., Coleman, D.C., Wiebe, W.J., 1998. Prokaryotes: the unseen majority. Proc. Nat. Acad. Sci. v. 95, 6578–6583.